Arch. Metall. Mater. **68** (2023), 3, 861-868

DOI: https://doi.org/10.24425/amm.2023.145448

E. GERÇEKCIOĞLU[1*], M. ALBAŞKARA[2]

MULTI-RESPONSE OPTIMIZATION OF ELECTRICAL DISCHARGE MACHINING OF 17-4 PH SS USING TAGUCHI-BASED GREY RELATIONAL ANALYSIS

Multiple response optimization of the machining of 17-4 PH stainless steel material, which is difficult to process with traditional methods, with EDM was made by Taguchi-based grey relational analysis method. Surface roughness (Ra), material removal rate (MRR), and electrode wear rate (EWR) were the responses, while current, pulse-on time, pulse-off time, and voltage were chosen as process parameters. According to the multi-response optimization, the experiment level that gave the best result was A1B2C2D2. Optimum machining outputs were found as A1B3C1D1 using the Taguchi method. As a result of the Taguchi analysis and ANOVA, it was determined that the significant parameters according to multiple performance characteristics were current (56.22%) and voltage (22.40%). The surfaces of the best GRG and optimal sample were examined with XRD, SEM and EDX analysis and the effects on the surfaces were compared.

Keywords: EDM; 17-4 PH SS; Taguchi-based Grey Relational Analysis; ANOVA; Surface Characterization

1. Introduction

17-4 PH stainless steel is a frequently used material in aerospace, defence, chemical, and food industries showing superior corrosion properties and high strength properties [1-3]. Cu particles of 4% wt. in the material structure increase the hardness and strength values of the material. It is impossible to machine 17-4 PH stainless steel with traditional machining methods due to its high hardness values [4-9]. Additionally, the high temperature released during traditional machining methods causes grain coarsening of Cu and negatively affects the mechanical properties of the material [10]. Therefore, it is important to machine 17-4 PH stainless steel with non-traditional methods.

EDM is one of the most used non-traditional machining methods to remove materials from hard-to-machine materials to produce molds, dies, aerospace and automotive parts, etc. In the EDM method, which uses electrical discharges to machine materials, chips are removed from a conductive workpiece by applying a spark at regular intervals through the electrode. Since there is no contact between the electrode and the workpiece in EDM, mechanical shearing forces do not occur on the workpiece, so mechanical stresses and distortions do not occur on the workpiece [11-14]. 17-4 PH material stands out as a suitable candidate material for machining with EDM since the surface quality can be improved to the desired extent and mechanical and thermal deteriorations do not occur in the material during EDM.

Experimental design and analysis methods based on mathematical models are frequently used when performing optimization studies in EDM. Muthuramalingam and Mohan (2013) machined AISI 202 stainless steel to investigate the effect of discharge current, gap voltage, and duty factor in EDM. They performed the experiments with the L27 orthogonal array choosing the full factorial Taguchi design [15]. Majumder (2013) aimed to improve the prediction of AISI 316LN stainless steel with EDM using fuzzy logic and particle swarm optimization. Pulse current, pulse-on time, and pulse-off time were input parameters; MRR and EWR were outputs [16]. Sharif et al. (2015) machined 316L stainless steel with die-sinking EDM using current, voltage, pulse-on time, and pulse-off time parameters. After machining, the results of MRR, electrode wear rate (EWR), SR, and dimensional accuracy (DA) were analysed with a mathematical model and ANOVA (analysis of variance) [17]. Rao et al. (2021) machined AISI D2 steel with EDM using pulse-on time, voltage, and peak current parameters according to Taguchi L9 orthogonal array. Output responses were MRR, TWR, and SR. ANOVA and Technique for Order of Preference

[1] ERCIYES UNIVERSITY, MECHANICAL ENGINEERING DEPARTMENT, KAYSERI, TURKEY
[2] AFYON KOCATEPE UNIVERSITY, İSCEHISAR VOCATIONAL SCHOOL, AFYONKARAHISAR, TURKEY
* Corresponding author: gercek@erciyes.edu.tr

by Similar to Ideal Solution (TOPSIS) analyses were performed to calculate the ideal parameters required for machining AISI D2 steel [18].

Taguchi experimental design is a method that allows conducting studies with less experimentation and low cost [19-25]. However, when analyses are made with the Taguchi experimental design, the effects of parameters on outputs are investigated separately. The highest S/N ratio for each parameter is the optimum level of that parameter. However, a level that is best for one output may be the worst level for another output [26]. However, in industrial manufacturing processes, manufacturing is not usually made for a single output. There are many different methods for multi-objective optimization studies [27-31].

Grey relational analysis (GRA) is a frequently used method for optimizing multiple outputs in machining studies. Saedon et al. (2014) machined the titanium alloy with the WEDM method. They carried out multi-objective optimization studies aiming for minimum surface roughness, high cutting speed, and material removal rate with Taguchi-based grey relational analysis [32]. Sarıkaya et al. (2015a) machined AISI 1050 steel by milling and carried out multi-optimization studies of vibration signals, cutting force, and surface roughness parameters. [33]. Sarıkaya et al. (2015b) machined cobalt-base superalloy Haynes 25, a difficult-to-cut material using Taguchi-based grey relational analysis. They investigated the effect of cutting fluid, fluid flow rate, and cutting speed parameters using Taguchi L9 orthogonal array and obtained optimum multi-response optimization results. [34]. Banh et al. (2017) machined CT3 steel with EDM using titanium powder. They conducted multi-objective optimization studies by investigating the material removal rate, tool wear rate, surface roughness, and microhardness outputs with Taguchi and GRA. [35]. Zerti et al. (2018) processed AISI D3 steel/mixed ceramic material by Taguchi L18 experimental design and performed multi-optimization studies with GRA. The effective process parameters were determined by ANOVA [36]. Uzun (2019) processed vermicular graphite cast iron material by milling, which was austempered at two different temperatures and in three different times. The effects of tool wear, cutting forces, and surface roughness parameters were investigated with the Taguchi experimental design. The most suitable experiment was found by multi-optimizing the results of tool wear, cutting force, and surface roughness. The effective parameters in processing were found with the help of ANOVA [37]. Jeyaprakash et al. (2020), who processed carbon fiber reinforced polymer material by micro-drilling method, investigated the effect of cutting speed and feed rate on entrance diameter, exit diameter, entrance circularity, and taper angle. Optimum levels were found by Taguchi-based GRA and effective parameters were found by ANOVA [38]. Gugulothu et al. (2020) examined Ti-6Al-4V alloy with multiple responses using grey relational analysis. The responses were material removal rate (MRR), surface roughness (Ra), and recast layer thickness (RLT), whereas process parameters were discharge current, pulse on time, pulse off time, and graphite powder concentration (g/l). The best machining level was found with Taguchi-based GRA and the effective parameters were found with the help of ANOVA. [39]. Phan et al. (2020) machined SKD 11 high-chromium tool steel with EDM and made multi-objective optimization with Taguchi-based GRA. The parameter level and optimum machining parameters that give the best results for MRR, SR, microhardness, and average white layer thickness outputs were found [40]. Kajendirakumar et al. (2021) machined D3 tool steel with EDM using the GRA multi-objective optimization method. They determined the best experimental result and the order of contribution of the parameters [41]. Kalyanakumar et al. (2021) investigated multi-mode machining parameters of EN24T lathe based on GRA. The experimental design was made according to Taguchi L9 orthogonal array. The effective parameters and contribution rank of the parameters were determined by Taguchi analysis and ANOVA [42].

The best machining parameters for 17-4 PH stainless steel were determined by multi-objective optimization of surface roughness (Ra), material removal rate (MRR) and electrode wear rate (EWR). Thus, multiple performance optimization studies were carried out for the 17-4 PH SS which is frequently used in the industry. In addition, in the studies conducted for EDM optimization in the literature, the surface condition after machining is not investigated. This situation poses a problem due to the importance of the usage areas of the material. In this study, the state of the machining surfaces of the best and optimal GRG samples was investigated in detail by XRD, SEM, and EDX analysis. Thus, besides machining optimization, the surface condition after machining was also examined and the necessary information was obtained for the use of 17-4 PH stainless steel during and after processing.

2. Experimental

2.1. Material and machining conditions

The chemical composition and XRF results of the 17-4 PH stainless steel material used in EDM studies are given in TABLE 1 and TABLE 2, respectively. As the tool material, wt 0.1% zirconium and wt 1% chromium alloy copper electrodes, which are more durable than pure copper, were used. The EDM setup where the machining is performed is shown in Fig. 1.

TABLE 1

Chemical composition of 17-4 PH stainless steel (wt. %)

C	Mn	Si	P	S	Cr	Ni	Cu	Nb+Ta	Fe
0.07	1.00	1.00	0.040	0.030	15.0 17.5	3.0 5.0	3.0 5.0	0.15 0.45	Balance

TABLE 2

XRF analysis of 17-4 PH stainless steel (wt. %)

Mn	Si	P	Cr	Ni	Cu	Nb+Ta	Fe
0.45	0.43	0.03	15.72	4.53	3.11	0.29	Balance

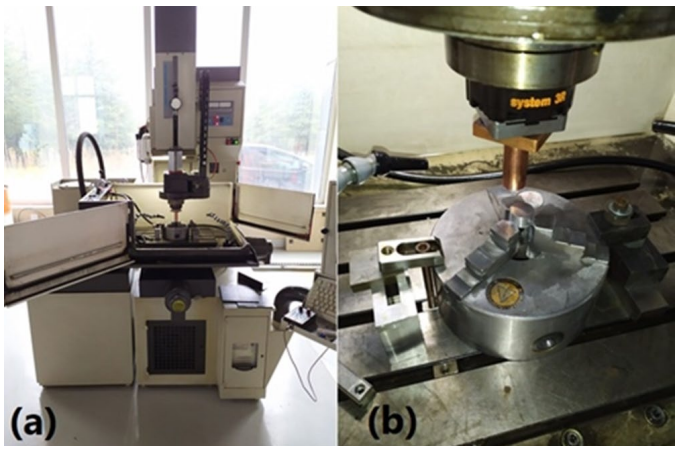

Fig. 1. a) EDM setup, b) sample fixed to the bench

The surfaces of the samples were cleaned with sanding and polishing processes, reducing the effect of surface roughness before machining. The surface of the copper electrode was also polished so that the machining on the workpiece surface was smooth. The samples and copper electrodes were weighed before and after machining, and *MRR* and *EWR* calculations were made using Equation (1) and Equation (2) after machining. Hydrocarbon oil was used as the dielectric fluid. Each sample was machined for 30 minutes so that the *MRR* and SR (Ra) values in the samples could be measured at the same standards and the machining time would not affect the machining [43].

$$MRR = \frac{W_{s1} - W_{s2}}{t} \tag{1}$$

$$EWR = \frac{W_{e1} - W_{e2}}{t} \tag{2}$$

The pre-and post-machining weights of the sample and the electrode are W_{s1} and W_{s2} and W_{e1} and W_{e2}, respectively. t is the machining time. Surface roughness values were measured by taking the average roughness (*Ra*) measurements from 10 regions on the surface of each sample with an optical profilometer (Fig. 2).

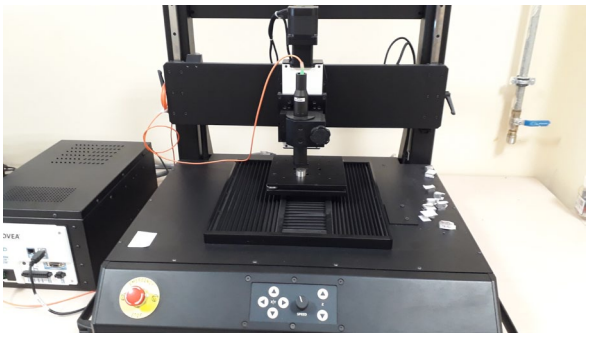

Fig. 2. Optical profilometer device with a sample

2.2. Taguchi Experimental Design

The Taguchi experimental design which is created by selecting the L9 orthogonal array for four parameters and three levels is given in TABLE 3 and TABLE 4, respectively. Current, pulse-on time (T_{on}), pulse-off time (T_{off}), and voltage parameters to be used in the experimental design are the parameters that are frequently used and affect the machining the most [11-13,44].

TABLE 3

Machining parameters and levels

Machining Parameters	Symbol	Level 1	Level 2	Level 3
Current (A)	A	7	12	22
Pulse-on Time (µs)	B	12	25	50
Pulse-off Time (µs)	C	12	25	50
Voltage (V)	D	40	60	100

TABLE 4

L_9 Taguchi experimental design

Exp. No.	L9 Orthogonal Array Design				A	B	C	D
1	1	1	1	1	7	12	12	40
2	1	2	2	2	7	25	25	60
3	1	3	3	3	7	50	50	100
4	2	1	2	3	12	12	25	100
5	2	2	3	1	12	25	50	40
6	2	3	1	2	12	50	12	60
7	3	1	3	2	22	12	50	60
8	3	2	1	3	22	25	12	100
9	3	3	2	1	22	50	25	40

In Taguchi-based grey relational analysis, S/N ratios corresponding to output results are found first. The "higher the better" for *MRR* and "lower the better" for (*Ra*) and *EWR* are calculated with the help of Equation (3) and Equation (4), respectively.

$$\frac{S}{N} = -10\log\frac{1}{n}\sum_{i=1}^{n} y^2 \tag{3}$$

$$\frac{S}{N} = -10\log\frac{1}{n}\sum_{i=1}^{n}\frac{1}{y^2} \tag{4}$$

2.3. Grey Relational Analysis

In the grey relational analysis, S/N ratios are first normalized between zero and one. The results are normalized using "higher the better" (Eq. 5) for *MRR* and "smaller the better" (Eq. 6) for *EWR* and *Ra*.

$$x_i(p) = \frac{X_i^0(p) - \min X_i^0(p)}{\max X_i^0(p) - \min X_i^0(p)} \tag{5}$$

$$x_i(p) = \frac{\max X_i^0(p) - X_i^0(p)}{\max X_i^0(p) - \min X_i^0(p)} \tag{6}$$

$X_i(p)$ is the normalized value calculated by transforming. $X_i^0(p)$ is the response value of aforementioned experiment number. $\max X_i^0(p)$ and $\min X_i^0(p)$ are the maximum and minimum values observed in the experiments. By subtracting the normalized

values from 1, deviation sequence (DS) values are found. Then, the grey relational coefficients (GRC) of each parameter are calculated using Equation 7. The value of ξ is chosen between 0-1. Usually, a value of 0.5 is a suitable value.

$$\xi_i(p) = \frac{\Delta_{\min} + \xi\Delta_{\max}}{\Delta_{0i}(p) + \xi\Delta_{\max}} \tag{7}$$

$$\Delta_{0i}(p) = \left| X_o(p) - X_j(p) \right| \tag{8}$$

$\Delta_{0i}(p)$ is the difference of the absolute value between $X_0(p)$ and $X_i(p)$. $\Delta_{\min}$ and $\Delta_{\max}$ are, respectively, the minimum and maximum values of the absolute differences of sequences. Grey relational grade (GRG) values are calculated using Equation 9. from the GRC values according to the number of parameters.

$$\gamma_i = \frac{1}{n}\sum_{p=1}^{n} \xi_i(p) \tag{9}$$

3. Results and Discussions

3.1. Grey relational analysis results

Surface roughness (*Ra*), electrode wear rate (*EWR*), and material removal rates (*MRR*) normalized values between 0 and 1 are given in TABLE 5, and deviation sequence, grey relational coefficient (GRC), and grey relational grade (GRG) values are given in TABLE 6. As can be seen from TABLE 5, *MRR* increased as current and pulse-on time increased and pulse-off time and voltage decreased. This is because as the current and T_{on} increase, the sparks between the tool and the workpiece increase and the discharge time increases. As current and T_{on} increased, surface roughness (*Ra*) also increased. This is because larger pieces of material break off with high and prolonged current discharges. In this case, pits and hills increase on the surface and a rougher structure is formed. *EWR* increased as the current increased. As the voltage decreased, visible spark increases occurred during machining. This suggests that the tool material erodes more as the voltage decreases.

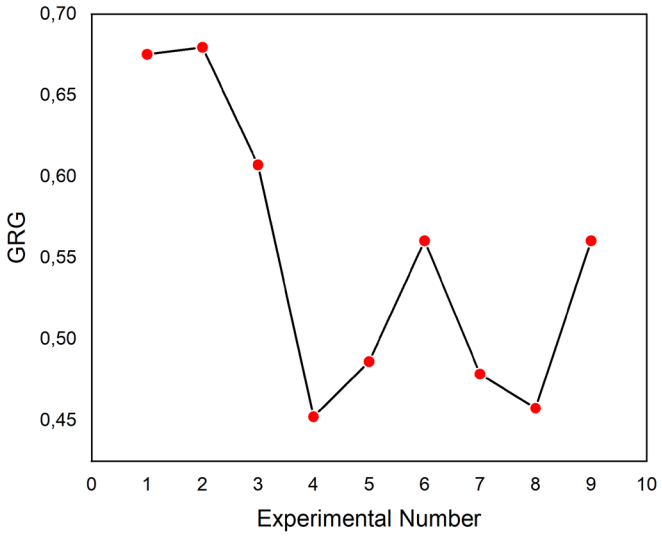

Fig. 3. GRG vs. experimental number

TABLE 5

Experimental and S/N results

Exp. No.	SR-Ra (µm)	S/N SR	EWR (mg/min)	S/N EWR	MRR (mg/min)	S/N MRR	Nor SR	Nor EWR	Nor MRR
1	2.126	–6.549	1.067	–0.561	11.824	21.455	1.000	0.763	0.061
2	2.522	–8.036	0.400	7.959	22.223	26.936	0.752	0.981	0.274
3	3.050	–9.686	0.367	8.714	9.854	19.872	0.476	1.000	0.000
4	2.773	–8.860	7.800	–17.842	15.101	23.580	0.614	0.321	0.144
5	3.577	–11.070	11.467	–21.189	90.906	39.172	0.244	0.235	0.748
6	4.182	–12.428	4.500	–13.064	154.264	43.765	0.017	0.443	0.926
7	2.744	–8.769	33.033	–30.379	51.022	34.155	0.629	0.000	0.554
8	3.543	–10.988	17.600	–24.910	72.047	37.152	0.258	0.140	0.670
9	4.232	–12.531	24.667	–27.842	192.051	45.668	0.000	0.065	1.000

TABLE 6

Grey relational results

Exp. No.	DS SR	DS EWR	DS MRR	GRC SR	GRC EWR	GRC MRR	GRG	Rank
1	0.000	0.237	0.939	**1.000**	0.678	0.348	0.675	2
2	0.248	0.019	0.726	0.668	0.963	0.408	0.680	1
3	0.524	0.000	1.000	0.488	**1.000**	0.333	0.607	3
4	0.386	0.679	0.856	0.564	0.424	0.369	0.452	9
5	0.756	0.765	0.252	0.398	0.395	0.665	0.486	6
6	0.983	0.557	0.074	0.337	0.473	0.871	0.561	5
7	0.371	1.000	0.446	0.574	0.333	0.528	0.479	7
8	0.742	0.860	0.330	0.403	0.368	0.602	0.457	8
9	1.000	0.935	0.000	0.333	0.348	**1.000**	0.561	4

As can be seen in TABLE 6 and Fig. 3, the experiment level that gives the best results is A1B2C2D2 and the first three experiments with low *Ra* and *EWR* have the best ranking, although their *MRR* values are low. This is because *EWR* and *Ra* give good results at lower current values. Thus, the first three experiments with the lowest current yielded the optimum multiple test outputs. The ninth experiment with the highest *MRR* was the fourth best result due to the high *Ra* and *EWR*.

By performing the Taguchi analysis with GRG values, mean GRG values corresponding to each level of each parameter were found and given in the response table in TABLE 7. In Fig. 4, mean GRG values corresponding to the levels of machining parameters are given. The highest GRG value is the optimal level. As can be seen in TABLE 7 and Fig. 4, the parameters that most affect multiple machining outputs are current and voltage. The impact of T_{on} and T_{off}, on the other hand, is limited but cannot be ignored.

TABLE 7

Response Table for Means

Level	Current	T_{on}	T_{off}	Voltage
1	**0.6540**	0.5354	**0.5644**	**0.5740**
2	0.4997	0.5411	0.5641	0.5729
3	0.4989	**0.5761**	0.5240	0.5056
Delta	0.1551	0.0407	0.0405	0.0684
Rank	1	3	4	2

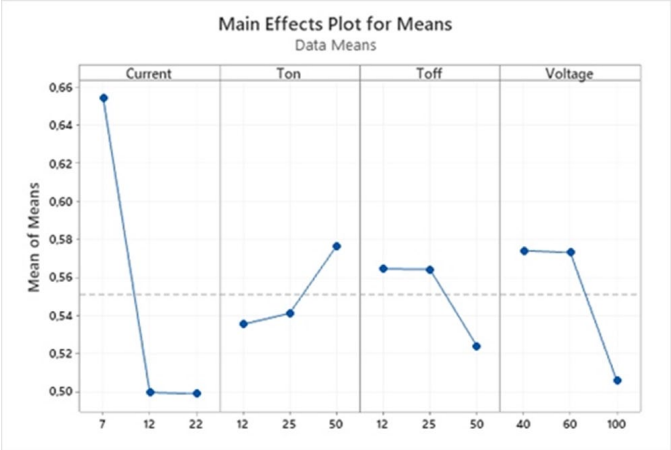

Fig. 4. GRA mean plot

3.2. Predict and optimization results

The best level of each parameter was selected from TABLE 7. and Fig. 4 to determine the optimum machining parameters. The higher the GRG value is, the better the obtained multiple machining results are. The predicted GRG result was calculated with the help of Equation (10). Therefore, the optimum machining parameters were determined as A1B3C1D1 for multiple output optimization. Machining studies were performed at level 1 (7A) for current, level 3 (50 µs) for T_{on}, level 1 (12 µs) for T_{off}, and level 1 (40 V) for voltage and compared with the best multiple GRG result. As can be seen from TABLE 8, although the outputs of the samples machined in optimum parameters do not give the best results in any parameter, the best overall GRG result is obtained. The predicted and experimental GRG values show very close values. There is a tiny difference (0.005) between the predicted and experimental GRG values. A better GRG result than the best GRG result of the initial experiments was found in the machining condition at optimal machining parameters. As a result, it was determined that the optimum machining parameters improved the multiple machining outputs and increased the GRG value significantly.

$$\gamma_{predicted} = \gamma_m \sum_{i=1}^{p} (\gamma_i - \gamma_m) \tag{10}$$

$\gamma_{predicted}$ is the GRG value of the estimated optimal processing parameters. γ_m is the total mean of the GRG. γ_i is the mean GRG value at the optimal level of the parameters.

TABLE 8

Optimal predict and experimental results

Outputs	Greatest GRG A1B2C2D2	Prediction A1B3C1D1	Experimental A1B3C1D1
SR	2.522	—	2.712
EWR	0.40	—	0.43
MRR	22.223	—	108.866
GRG	0.680	0.716	0.721

3.3. ANOVA (Analysis of Variance)

Analysis of variance (ANOVA) was performed using the pooling method, and the T_{off} parameter, which was the least affecting parameter, was excluded from the analysis. The values corresponding to the error were counted as the T_{off} value, which is the pooled parameter. The ANOVA results given in TABLE 9 gave similar results to the Taguchi analysis. The parameters that contribute most to the machining are current and voltage, respectively. The contribution of current to machining was calculated as 56.22%, and the effect of voltage as 22.40%. In order to understand whether the parameters are effective, the p-value must be below 0.05. The fact that the *p*-value of the current, which is the most significant parameter in machining, is 0.023 explains this situation.

TABLE 9

ANOVA results for GRG (%95 confidence level)

Source	DF	Sum of Squares	Means Square	F-Value	P-Value	Percentage (%)
Current	2	0.040311	0.020155	42.32	0.023	56.22
T_{on}	2	0.014381	0.007191	15.10	0.062	20.06
T_{off}^{*}	2	0.000953	0.000476	—	—	1.33
Voltage	2	0.016058	0.008029	16.86	0.056	22.40
Total	8	0.071703				

*: Pooled Parameter R-square = %98.67

According to the results obtained from ANOVA and the Taguchi analysis, the effect of current and voltage, which are the two parameters that most affect multiple machining outputs, on GRG is shown in Fig. 5. It is clearly seen that the GRG value increases as the voltage and current decrease. As the current increased to 22A, some GRG increase was seen due to the increase in *MRR*.

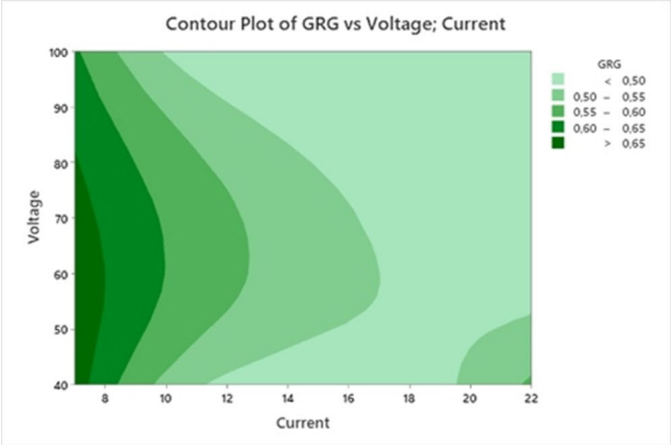

Fig. 5. GRG vs. voltage and current contour plot

3.4. XRD and SEM Analysis

XRD results of the best GRG (A1B2C2D2) and optimal sample (A1B3C1D1) are given in Fig. 6. Peaks are seen in both samples at the same 2θ scanning angles. It is understood that the change in machining parameters does not cause any phase transformation on the machining surfaces. It is thought that the difference in the sizes of the peaks is due to the growth and increase of the crystallite sizes of the phases formed on the machining surface.

SEM images of the sample with the best GRG value and the sample machined in optimal parameters are given in Fig. 7. Very small and capillary microcracks are seen on the surface of the machined sample at the best GRG value (Fig. 7a). Due to the very low material removal, the surface is relatively smooth.

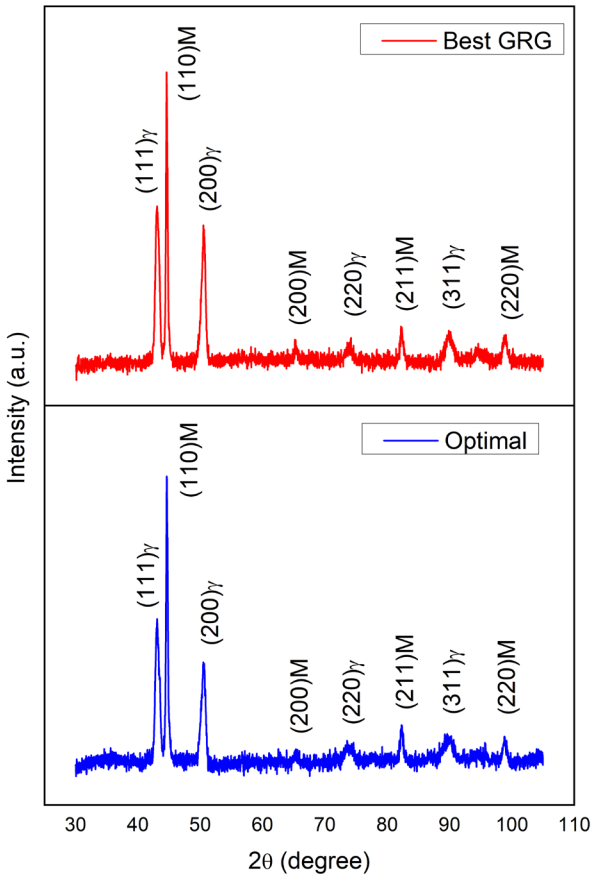

Fig. 6. XRD results of best GRG and optimal samples

The average surface roughness value (2.522 µm) of this experiment also explains this situation. Craters, few and small recast regions are seen in the SEM image of the sample machined at optimal parameters (Fig. 7b). This is due to the increase in electrical discharges applied to the workpiece and sparking between the workpiece and the tool as a result of the increase in T_{on} and decrease in voltage. As a result, a very significant increase in MRR was seen in the optimal machining sample. Along with well-machined areas on the surface, some areas that partially increased the roughness were observed. This resulted in a partial increase in surface roughness (2.712 µm).

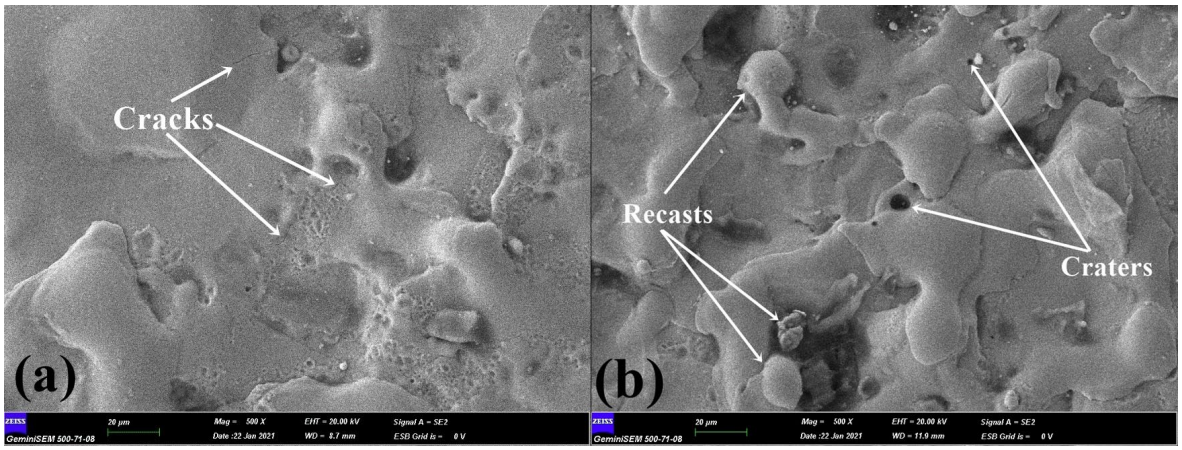

Fig. 7. (a) SEM images of the best GRG, (b) machined at optimal parameters

Elemental composition on the machining surfaces was determined by EDX analysis. Since light elements such as carbon (C) and oxygen (O) have lower photon energy than heavy elements, EDX analysis may not give very accurate numerical values for light elements. However, it can be used for comparison to determine the effect of different parameters [45]. EDX results of Best GRG and optimal machining parameters are given in TABLE 10 and energy levels are given in Fig. 8. As can be seen from the analysis results, the "Fe" ratio increases and the "C" ratio decreases on optimal machined surface. As the T_{on} increases, the "Fe" ratio increases and the "C" ratio decreases, as it provided more machining and did not allow the carbon to adhere to the surface. Oxygen was also found on the surface. This is thought to be due to the oxidation that occurs during resolidification of the debris [46,47].

TABLE 10

EDX analysis results of best GRG and optimal machined samples (wt. %)

Sample	Fe	C	Cr	Ni	Cu	Si	O
Best	58.31	19.03	14.62	2.88	2.30	0.36	2.50
Optimal	62.51	13.40	15.74	3.06	2.45	0.46	2.38

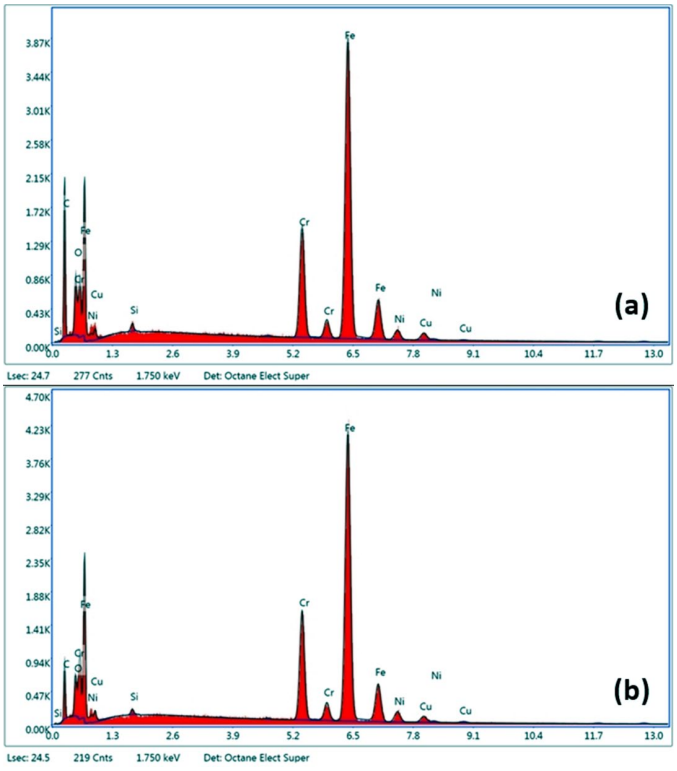

Fig. 8. (a) EDX graph of the best GRG, (b) machined at optimal parameters

4. Conclusions

In the present study, 17-4 PH stainless steel material was machined by EDM and GRA studies were carried out with the help of the Taguchi orthogonal array. Multiple performance characteristics of MRR, Ra, and EWR outputs were investigated. Optimization studies were carried out by predicting optimal machining levels and calculating experimental GRGs. The characterization studies of best GRG and optimal machined samples were carried out and their surface conditions after machining were investigated. The best multiple machining rank was determined. According to GRA, the best multiple machining outputs were seen in the second experiment (A1B2C2D2). By performing the Taguchi analysis, it was determined that the parameters that affected the multiple machining output the most were current and voltage, respectively. The optimal level of each parameter was determined with the help of the Taguchi analysis. Accordingly, the optimal results of multiple machining outputs were found to be A1B3C1D1. Predicted and experimental results were obtained by performing optimal machining studies. A better GRG result than the best GRG result of the initial experiments was found in the machining condition at optimal machining parameters. Analysis of variance (ANOVA) studies were conducted to determine the parameters and contribution rates that most affected the machining. The most significant parameters were current and voltage, respectively, as in the Taguchi analysis. XRD results of the best GRG and optimal samples showed that the change in machining parameters did not cause phase transformation on the machining surface. SEM images of the sample with the best GRG value and the optimal machining sample were examined. Well-machined regions were seen on the surface of the workpiece with the best GRG value. On the other hand, deformations were detected in the optimal machining sample which resulted from the increase in electrical discharges between the tool and the workpiece and caused a relatively increased roughness. The EDX results showed that as the T_{on} increased, Fe increased and C decreased on the material surface. In the future, optimization studies and characterization studies will be carried out together and, in more detail, so that the post-machining conditions of critical materials whose usage areas are important will be better observed.

Acknowledgement

This study was supported by the Erciyes University Scientific Research Projects Coordination Unit under grant number FDK-2020-9339.
The authors, also, would like to thank Mr. Hüsamettin Ertürk from İscehisar Vocational School for his valuable support for the softwares.

REFERENCES

[1] N. Hsiao, C.S. Chiou, J.R. Yang, Mater. Chem. Phys. **74**, 134-142 (2002). DOI: https://doi.org/10.1016/S0254-0584(01)00460-6
[2] Gopalakannan, T. Senthilvelan, J. Miner. Mater. Char. Eng. **11**, 685-690 (2012). DOI: https://doi.org/10.4236/jmmce.2012.117053
[3] A. Thakur, M. Tak, R.G. Mote, Procedia. Manuf. **34**, 355-361 (2019). DOI: https://doi.org/10.1016/j.promfg.2019.06.177

[4] S. Chandramouli, K. Eswaraiah, Mater. Today-Proc. **4**, 2040-2047 (2017). DOI: https://doi.org/10.1016/j.matpr.2017.02.049
[5] S. Chandramouli, K. Eswaraiah, Mater. Today-Proc. **5**, 5058-5067 (2018). DOI: https://doi.org/10.1016/j.matpr.2017.12.084
[6] S. Pasebani, M. Ghayoora, S. Badweb, H. Irrinki, S.V. Atre, Addit. Manuf. **22**, 127-137 (2018). DOI: https://doi.org/10.1016/j.addma.2018.05.011
[7] P.D. Nezhadfar, E. Burford, K. Anderson-Wedge, B. Zhang, S. Shao, S.R. Daniewicz, N. Shamsaei, Int. J. Fatigue. **123**, 168-179 (2019). DOI: https://doi.org/10.1016/j.ijfatigue.2019.02.015
[8] L. Carneiro, B. Jalalahmadi, A. Ashtekar, Y. Jiang, Int. J. Fatigue **123**, 22-30 (2019). DOI: https://doi.org/10.1016/j.ijfatigue.2019.02.006
[9] M. Albaskara, Z. Arsoy, E. Gerçekcioğlu, J. Charact. **1** (2), 50-60 (2021). DOI: https://doi.org/10.29228/JCHAR.50779
[10] Y. Sun, R.J. Hebert, M. Aindow, Mater. Design **156**, 429-440 (2018). DOI: https://doi.org/10.1016/j.matdes.2018.07.015
[11] K.H. Ho, S.T. Newman, Int. J. Mach. Tool. Manu. **43**, 1287-1300 (2003). DOI: https://doi.org/10.1016/S0890-6955(03)00162-7
[12] M. Kiyak, O. Çakır, J. Mater. Process. Tech. 191, 141-144 (2007). DOI: https://doi.org/10.1016/j.jmatprotec.2007.03.008
[13] N.M. Abbas, D.G. Solomon, M.F. Bahari, Int. J. Mach. Tool. Manu. *47*, 1214-1228, (2007). DOI: https://doi.org/10.1016/j.ijmachtools.2006.08.026
[14] J.E. Abu Qudeiri, A. Saleh, A. Ziout., A.H.I. Mourad, M.H. Abidi, A. Elkaseer, Materials **12** (6), 907 (2019). DOI: https://doi.org/10.3390/ma12060907
[15] T. Muthuramalingam, B. Mohan, Mater. Manuf. Process. **28** (4), 375-380 (2013). DOI: https://doi.org/10.1080/10426914.2012.746700
[16] A. Majumder, J. Mech. Sci. Technol. **27** (7), 2143-2151 (2013). DOI: https://doi.org/10.1007/s12206-013-0524-x
[17] S. Sharif, W. Safiei, A.F. Mansor, M.H.M. Isa, R.M. Saad, Procedia. Manuf. **2**, 147-152 (2015). DOI: https://doi.org/10.1016/j.promfg.2015.07.026
[18] K.M. Rao, D.V. Kumar, K.C. Shekar, B. Singaravel, Mater. Today-Proc. **46** (1), 701-706 (2021). DOI: https://doi.org/10.1016/j.matpr.2020.12.067
[19] R.K. Roy, Design of Experiments Using the Taguchi Approach, John Wiley & Sons, New York (2001).
[20] M. Rahang, P.K. Patowari, Mater. Manuf. Process. **31**, 422-431 (2016). DOI: https://doi.org/10.1080/10426914.2015.1037921
[21] K. Aslantaş, E. Ekici, A. Çiçek, Measurement **128**, 419-427 (2018). DOI: https://doi.org/10.1016/j.measurement.2018.06.066
[22] P. Sivaiah, D. Chakradhar, Measurement **134**, 142-152 (2019). DOI: https://doi.org/10.1016/j.measurement.2018.10.067
[23] M.R. Kumar, A. Krishnaiah, R.S. Kalva, Mater. Today-Proc. **5**, 27269-27276 (2018). DOI: https://doi.org/10.1016/j.matpr.2018.09.043
[24] S.V. Narayanan, D.M. Benjamin, M.V. Hariharan, R. Keshav, D.S. Raj, Mach. Sci. Technol. **25** (2), 209-236 (2021). DOI: https://doi.org/10.1080/10910344.2020.1815037
[25] C. Moganapriya, R. Rajasekar, K. Ponapp, R. Venkatesh, R. Karthick, Arch. Metall. Mater. **62** (3), 1827-1832 (2017). DOI: https://doi.org/10.1515/amm-2017-0276
[26] J.L. Lin, C.L. Lin, Int. J. Mach. Tool. Manu. **42**, 237-244 (2002).
[27] H.N. Phan, T. Muthuramalingam, Silicon **13**, 2771-2783 (2021). DOI: https://doi.org/10.1007/s12633-020-00632-w
[28] H.N. Phan, T. Muthuramalingam, Silicon **13**, 1879-1885 (2021). DOI: https://doi.org/10.1007/s12633-020-00573-4
[29] E. Kuram, B. Özcelik, Measurement **46**, 6, 1849-1864 (2013). DOI: https://doi.org/10.1016/j.measurement.2013.02.002
[30] Y. Kuo, T. Yang, G.W. Huang, Eng. Optimiz. **40** (6), 517-528 (2018). DOI: https://doi.org/10.1080/03052150701857645
[31] M. Sivaraj, S. Rajkumar, S. Muthuraman, Mater. Today-Proc. **37**, 2, 1254-1263 (2021). DOI: https://doi.org/10.1016/j.matpr.2020.06.437
[32] J.B. Saedon, N. Jaafar, M.A. Yahaya, N.H. Saada, M.S. Kasim, Proc. Tech. **15**, 832-840 (2014). DOI: https://doi.org/10.1016/j.protcy.2014.09.057
[33] M. Sarıkaya, V. Yılmaz, H. Dilipak, Proc. Inst. Mech. Eng. Part B. **230** (6), 1049-1065 (2015). DOI: https://doi.org/10.1177/0954405414565136
[34] M. Sarıkaya, A. Güllü, J. Clean. Prod. **91**, 347-357 (2015). DOI: https://doi.org/10.1016/j.jclepro.2014.12.020
[35] T.L. Banh, H.P. Nguyen, C. Ngo, D.T. Nguyen, Proc. Inst. Mech. Eng. E: J. Process Mech. Eng. **232** (3), 281-298. DOI: https://doi.org/10.1177/0954408917693661
[36] O. Zerti, M.A. Yallese, A. Zerti, S. Belhadi, F. Girardin, Int. J. Ind. Eng. Comput. **9**, 173-194 (2018). DOI: https://doi.org/10.5267/j.ijiec.2017.7.001
[37] G. Uzun, Measurement **142**, 122-130 (2019). DOI: https://doi.org/10.1016/j.measurement.2019.04.059
[38] N. Jeyaprakash, C.H. Yang, D.R. Kumar, Mater. Today-Proc. **21** (3), 1425-1431 (2020). DOI: https://doi.org/10.1016/j.matpr.2019.08.212
[39] B. Gugulothu, G.K.M. Rao, M. Bezabih, Mater. Today-Proc. **46** (1), 89-98 (2021). DOI: https://doi.org/10.1016/j.matpr.2020.06.135
[40] P.H. Nguyen, T.L. Banh, K.A. Mashood, Arab. J. Sci. Eng. **45**, 5555-5562 (2020). DOI: https://doi.org/10.1007/s13369-020-04456-z
[41] S.V. Kajendirakumar, G.S. Kumar, P. Parameswaran, B.S. Kumar, Mater. Today-Proc. **37** (2), 1137-1139 (2021). DOI: https://doi.org/10.1016/j.matpr.2020.06.347
[42] S. Kalyanakumar, S.T. Chandy, K.T.A. Muhammed, P.S. Rohith, Mater. Today-Proc. **45** (7), 6193-6197 (2021). DOI: https://doi.org/10.1016/j.matpr.2020.10.508
[43] C.H.C. Haron, B.Md. Deros, A. Ginting, M. Fauziah, J. Mater. Process. Tech. **116**, 84-87 (2001).
[44] T. Rajmohan, R. Prabhu, G.S. Rao, K. Palanikumar, Procedia. Eng. **38**, 1030-1036 (2012). DOI: https://doi.org/10.1016/j.proeng.2012.06.129
[45] M. Chakmakchi, A. Ntasi, W. D. Mueller, S. Zinelis, Dent. Mater. **37**, 4, 588-596 (2021). DOI: https://doi.org/10.1016/j.dental.2021.01.012
[46] N. Natarajan, P. Suresh, Int. J. Adv. Manuf. Technol. **77**, 1741-1750, (2014). DOI: 10.1007/s00170-014-6494-z
[47] K.K. Saxena, S. Agarwal, S.K. Khare, Procedia. CIRP. **42**, 79-184 (2016). DOI: https://doi.org/10.1016/j.procir.2016.02.267